Multi-physics Modeling of Coal Gasification Processes in a Well-Stirred Reactor with Detailed Chemistry

Jian Xu[1], Li Qiao[2]*, and Jay Gore[3]
[1,2]School of Aeronautics and Astronautics, Purdue University, West Lafayette, IN, 47907
[3]School of Mechanical Engineering, Purdue University, West Lafayette, IN, 47907

1 Instruction

Fuel synthesis through coal gasification can potentially provide a solution to the increasing demand of energy and transportation fuels. Understanding the complex chemical processes in coal gasification, both experimentally and computationally, has received increasing interest in recent years. In terms of modeling coal gasification processes, previous work have mainly focused on three areas ─ single coal particle gasification[1-3,] one-dimensional coal gasification[4-7], and Computational Fluid Dynamics (CFD) coal gasification[8-12.] CFD modeling of entrained flow reactors is extremely complex, involving gas-phase turbulent flow and particle-phase turbulent flow as well as particle-gas phase coupling, which is beyond the scope of the present study and thus will not be discussed here.

Previous studies have shown that several factors, including the detailed devolatilization kinetics, gas-phase reactions, char structure (through diffusion process) as well as char surface reactions, can all influence gasification behavior, especially at high pressures. The models in literature have mostly used simple kinetics or reactions and some reactions were assumed to be at equilibrium. The reaction rate has been mostly expressed in terms of one-step overall reaction rate, which may not be accurate enough. Additionally, multi-physics interactions between gas-phase and particle-phase were not carefully considered in these models. Some interactions that account for the mass and energy exchange between the two phases were even neglected. These studies indicate that a more detailed model that includes diffusion process, char structure, surface reactions, as well as interactions between the two-phase at the boundary, is needed for particles at the small scale of particle size. In particular, the interactions between the particle-phase and the surrounding gases should be carefully considered. Finally, gas-phase homogenous reactions and transport, which have shown to have an importance impact on the gasification behavior, should be better described using detailed chemistry, variable thermodynamic properties, and multi-component transport properties.

Motivate by this, we developed a multi-physics model with detailed gas-phase chemistry and a numerical code to simulate the complex gasification processes in a perfect-stirred reactor. The model considers gas-phase and particle-phase reactions as well as coupling including mass and energy exchanges between the two phases at various scales. The government equations for both phases were developed. Finally, numerical simulations were conducted to understand the gasification process at various operating conditions.

2 Model description

A multi-physics model with detailed chemistry was developed to simulate coal gasification processes in a well-stirred reactor. Figure 1 shows a schematic of the reactor. Carbon particles with diameter dp are uniformly distributed inside the reactor together with gaseous species. The pressure of the reactor remains constant, which means during the gasification process the volume increases due to

Correspondence to: lqiao@purdue.edu

thermal expansion and thus the number density of coal particles decreases but the total number of particles is conserved. We assume intense mixing occurs inside the reactor so that all gas-phase properties are uniform or spatially-independent. We also assume the temperature and number density of particles are uniform inside the reactor. However, there are mass, species and energy exchanges between individual particles and the surrounding gases, causing local non-equilibrium. These interactions are modeled on the particle scale. In other words, a single particle is modeled to include several mechanisms (surface heterogeneous reactions, diffusion process onto particle surface, and heat transfer between the particle and the surrounding gases). Moreover, the model developed for a single particle will represent all particles inside the reactor as we assume the mixture is well-stirred. For the gas-phase reactions, detailed kinetics, multi-component diffusion, and variable thermodynamic properties are considered. The governing equations of mass, species, and energy conservation for the gas-phase and the particle-phase are coupled to account for mass, species and energy exchange between the two phases. The transient gasification process will be computed until 99% of the coal particle is gasified.

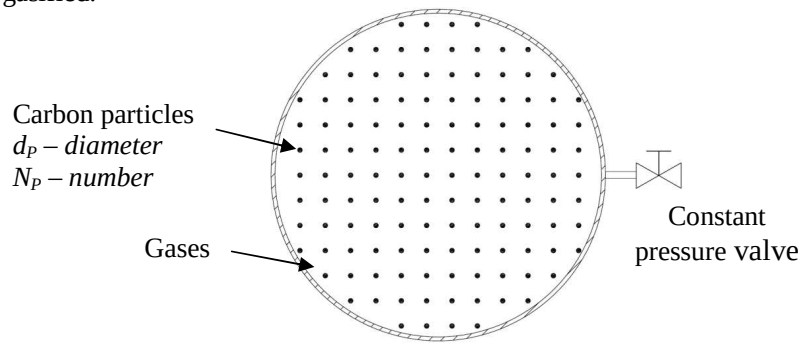

Figure1. Coal Gasification in a Well-Stirred Reactor.

A. Gas Phase Equations

The conservation equations of mass, species and energy for the gas phase are given as:

$$\frac{d(\rho_g V)}{dt} - V\sum \omega_i W_i = 0 \quad (1)$$

$$\rho_g \frac{dY_i}{dt} + Y_i \sum_{k=1}^{K} \omega_k W_k - \omega_i W_i - N_P R_{C,i} = 0 \quad (2)$$

$$\rho_g \frac{dT_g}{dt} + \left(\sum_k \omega_k W_k h_k - (S_{p-g} + S_h) * N_p \right) / \bar{C}_{p,g} = 0 \quad (3)$$

In Eq. (1), w_i is the production rate of species *i* because of gas-phase reactions and surface heterogeneous reactions. W_i is the molecular weight of species *i*. In Eq. (2), Y_i is the mass fraction of species i. N_p is the particle number density. $R_{C,i}$ is the production rate of species *i* because of the surface reactions which species *i* participates in. In Eq. (3), h_i is the enthalpy of species i. S_{p-g} represents enthalpy transfer between the two phases due to mass transfer. S_h is the convection heat transfer between the particle and its surrounding gases.

A detailed gas-phase reaction mechanism, GRI-Mech 1.2[13], is incorporated into the model, which includes 177 elementary reactions and 31 species. Other mechanisms were also used but the results shown here are based on GRI-Mech 1.2. The gas phase species are: H2, H, O, O2, OH, H2O, HO2, H2O2, C, CH, CH2, CH2(S) , CH3, CH4, CO, CO2, HCO, CH2O, CH2OH, CH3O, CH3OH, C2H, C2H2, C2H3, C2H4, C2H5, C2H6, HCCO, CH2CO, HCCOH, and N2. Multi-component transport properties and variable thermodynamic properties were adopted based on CHEMKIN format.

B. Particle Phase Equations

The mass and energy conservation equations of a single particle are expressed as

$$\frac{dm_p}{dt} - \rho_p A_p \frac{dr_p}{dt} = 0 \tag{4}$$

$$m_p C_{p,p} \frac{dT_p}{dt} - (Q_C + S'_{p-g} + S'_h) = 0 \tag{5}$$

In Eq. (5), Q_C is the gross heat by four surface reactions and is expressed as

$$Q_C = \dot{m}_{C,A} Q_{C,A} + \dot{m}_{C,B} Q_{C,B} + \dot{m}_{C,C} Q_{C,C} + \dot{m}_{C,D} Q_{C,D} \tag{6}$$

Where $\dot{m}_{C,A}$, $\dot{m}_{C,B}$, $\dot{m}_{C,C}$, $\dot{m}_{C,D}$ and $Q_{C,A}$, $Q_{C,B}$, $Q_{C,C}$, $Q_{C,D}$ are the carbon consumption rate and reaction heat of surface reactions A, B, C and D. These reactions are described in the following.

C. Char Surface reactions

Four heterogeneous reactions are assumed to take place at the surface of particles:

$$C + H_2O \rightarrow CO + H_2 \tag{A}$$

$$C + CO_2 \rightarrow 2CO \tag{B}$$

$$C + 2H_2 \rightarrow CH_4 \tag{C}$$

$$2C + O_2 \rightarrow 2CO \tag{D}$$

The reaction rate controlled by boundary layer diffusion is given by Eq. 7[14]. The reaction rate can be expressed as a function of the partial pressure of the gaseous reactant and the external surface area of the particle as Eq. 8[15].

$$\dot{m}_{C,j} = \frac{A_p D_i P W_c}{r_p R_u T_g} (X_i - X_{s,i}) \tag{7}$$

$$\dot{m}_{C,j} = k_{s,j} A_p (P X_{s,i})^n \tag{8}$$

Where, X_i and $X_{s,i}$ are the mole fractions of specie i (H_2O, CO_2, H_2 and O_2) in the gas-phase and at the particle surface respectively. $k_{s,j}$ is the rate constant of the surface reactions A, B, C and D. By eliminating $X_{s,i}$, the surface reaction rate can be obtained as:

$$\dot{m}_{C,j} = A_p k_{s,j} P X_i \left(\frac{D_i W_c}{k_{s,j} r_p R_u T_g + D_i W_c}\right) \tag{9}$$

3 Preliminary results

Numerical simulations were conducted at various operating conditions to gain a better understanding of the gasification processes and to identify the most influential parameters on gasification performance. The result shown in the following is a general case and the parameters used in the simulation are shown in Table 1.

Table 1: Initial conditions.

Initial gas temperature	$T_g = 1200K$	Initial particle temperature	$T_p = 1200K$
Gas pressure	$P = 10atm$	Density of particles	$\rho_p = 1.3g/cm^3$
Initial water concentration	$X_{H_2O} = 0.9$	Initial particle diameter	$d_p = 25\mu m$
Initial oxygen concentration	$X_{O_2} = 0.1$	Particle number density	$N_p = 55615/cm^3$

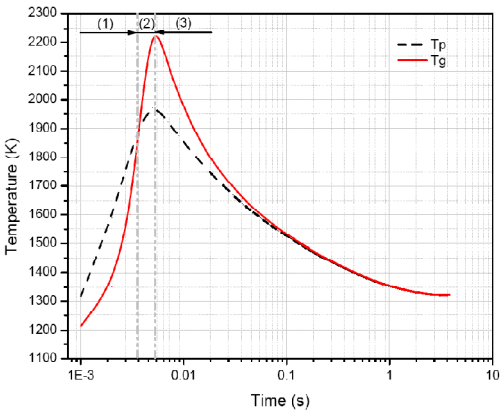

Figure 2. Profiles of gas and particle temperature.

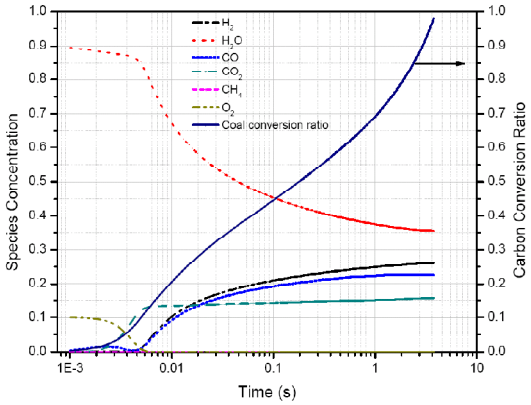

Figure 3. Profiles of species concentration and carbon conversion rate.

Figure 2 shows the temperature profiles of the gas phase and the particle phase as a function of time. The particle and gas temperatures increase rapidly to a maximum (T_p = *1970 K* and T_g = *2250 K*) in 0.005 second. T_p and T_g then decrease and remain the same after $t > 0.05s$. T_p is higher than T_g at the initial period ($t < 0.003s$), but becomes lower until an equilibrium is reached at $t = 0.05s$. The peaks of the temperatures take place at the point at which the oxygen is completely consumed, as can be seen in Fig. 3. In the initial period, oxidation of both the gas phase (mainly reactions $2CO+O_2 \rightarrow 2CO_2$ (E) and $2H_2+O_2 \rightarrow 2H_2O$ (F)) and the particle phase ($C+O_2=2CO$ (D)) take place. However, the rates of the gas phase reactions are much faster than those of solid-gas reactions. The gas-phase oxidation reactions are dominant in the presence of O_2. This explains why the peak temperature of T_g is higher than the peak of T_p because of larger heat release from the gas-phase oxidation reactions. Later, after oxygen is consumed, T_p and T_g reach the same value because of convective heat transfer between the particles and the gases.

Figure 3 shows the concentration profiles of six stable species as well as carbon conversion rate as a function of time. Note the simulation ends when 99% of carbon particles are gasified. The concentrations of intermediate and minor species are not shown, which are much lower than the stable species. The gasification process needs about 4.5 seconds to be complete. At $0s < t < 0.005s$, oxygen concentration falls to zero and CO concentration increases slightly first and then decreases to zero, while CO_2 concentration keeps increasing to over 10%. During this period, carbon surface oxidation reaction (D) and gas-phase reaction (E) are the dominant reactions which consumes most oxygen. At $t > 0.005s$ when O_2 is consumed and a peak temperature has been achieved, carbon surface reactions A, B and C become more important, particularly the carbon-steam reaction A, which causes the concentrations of CO and H_2 to increase and the concentration of H_2O to decrease.

To further understand the relative importance of the four surface reactions, the reaction rates of Reactions A, B, C, and D are plotted as a function of time in Fig. 4. During the initial period, the rate of $2C+O_2 \rightarrow 2CO$ reaction is much higher (100 times) than the rate of $C+H_2O \rightarrow CO+H_2$ reaction. After oxygen is depleted, the carbon-steam reaction becomes dominant, with a rate about 10 times higher than the rate of $C+CO_2 \rightarrow 2CO$ reaction. The reaction rate of $C+2H_2 \rightarrow CH_4$ reaction is much slower than the other two during the whole gasification process and thus can be neglected under present conditions. Based on Figs. 2-4, we can divide the gasification process into three stages: (1) carbon oxidation, (2) gas-phase oxidation, (3) carbon gasification, as noted in Fig. 2.

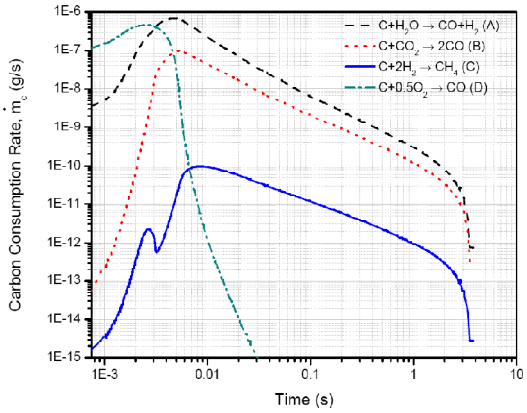

Figure 4. Profiles of carbon consumption rate.

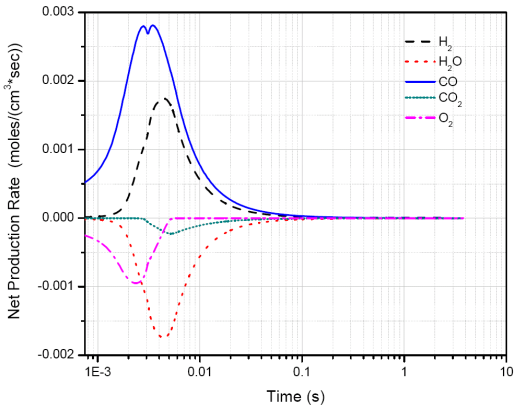

Figure 5. Net production rate of five species due to surface reactions on particle.

Figure 5 shows the net production rates of five species as a function of time as a result of surface reactions. The CO curve has two peaks. The first peak is due to $C+0.5O_2 \rightarrow CO$ reaction, and the second peak is due to $C+H_2O \rightarrow CO+H_2$ reaction. The first peak corresponds to a maximum consumption rate of O_2. And the second peak is approximately aligned with a maximum consumption rate of H_2O and a maximum production rate of H_2. At $t > 0.1s$, the rates of all species approach very low because of the temperature drop which lowers the reactivity.

Figure 6 shows the source terms in the particle and gas energy equations. For the purpose of comparison, all source terms are scaled with $\dot{m}_{C,A} Q_{C,A}$. As shown in Fig. 6, the heat released by reaction D ($C+0.5O_2 \rightarrow CO$) and the convective heat transfer between particles and surrounding gases are most important in the initial stage. The former increases the particle temperature and the latter increases the gas temperature by convection. After O_2 is consumed, the absorbed heat by reaction A ($C+H_2O \rightarrow CO+H_2$) and the convective heat transfer are most important. The absorbed heat by reaction B ($C+CO_2 \rightarrow 2CO$) increases, but the value is smaller than half of the absorbed heat by reaction A. The total enthalpy transfer due to mass transfer by the surface reactions is much smaller compared to the other source terms in the particle energy equation.

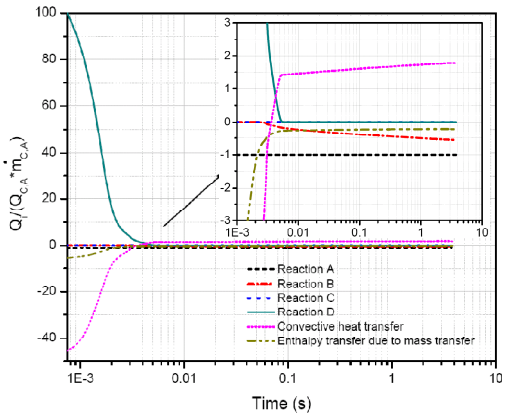

Figure 6. Comparison of the source terms in the particle energy equation.

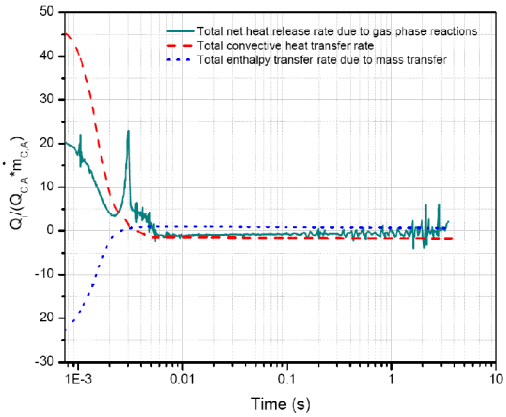

Figure 7. Comparison of the source terms in the gas energy equation.

Figure 7 shows a comparison of three source terms in the gas energy equation, including the total heat by gas-phase reactions, convective heat transfer, and enthalpy transfer due to mass transfer from the surface reactions. In the initial stage, convective heat transfer between the two phases is dominant. A peak of the total heat by gas-phase reactions occurs around $t = 0.003s$. Later during the gasification stage, the three source terms remain almost constant.

4 Conclusions

Following conclusions can be reached based on the present study: 1. With the presence of oxygen in the reactant mixture, the chemical process in the reactor can be divided into three stages: carbon oxidation, gas-phase oxidation, and carbon gasification. 2. In the first stage, the reaction rate of $C+0.5O_2 \rightarrow CO$ is much faster than the other surface reactions. In the later stages, $C+H_2O \rightarrow CO+H_2$ reaction dominates the consumption of carbon, with a rate about 10 times higher than the rate of $C+CO_2 \rightarrow 2CO$ reaction. 3. In the particle energy equation, reaction heat by $C+0.5O_2 \rightarrow CO$ and convective heat transfer between particles and the surrounding gases are most important in the initial stage. Later when O_2 is consumed, reaction heat by $C+H_2O \rightarrow CO+H_2$ and convective heat transfer are most important. 4. In the gas energy equation, convective heat transfer between the two phases is dominant at the initial stage. Later during the gasification stage, the three source terms (gas phase reaction heat, convection heat transfer and enthalpy heat transfer due to mass exchange) have very similar order of magnitude and remain almost constant.

References

[1] Srinivas, B. and N.R. Amundson, "A single-particle char gasification model," Aiche Journal, Vol. 26, No. 3, 1980, pp. 487-496.
[2] Haynes, H.W., "An improved single-particle char gasification model," Aiche Journal, Vol. 28, No. 3, 1982, pp. 517-521.
[3] Samuilov, E.V., M.F. Faminskaya, and E.S. Golovina, "Model and calculation of the gasification of a single carbon particle," Combustion Explosion and Shock Waves, Vol. 40, No. 1, 2004, pp. 77-84.
[4] Govind, R. and J. Shah, "Modeling and simulation of an entrained flow coal gasifier," Aiche Journal, Vol. 30, No. 1, 1984, pp. 79-92.
[5] Ni, Q.H. and A. Williams, "A simulation study on the performance of an entrained-flow coal gasifier," Fuel, Vol. 74, No. 1, 1995, pp. 102-110.
[6] Vamvuka, D., E.T. Woodburn, and P.R. Senior, "Modeling of an entrained flow coal gasifier. 1. Development of the model and general predictions," Fuel, Vol. 74, No. 10, 1995, pp. 1452-1460.
[7] Liu, G.S., et al., "Modelling of a pressurised entrained flow coal gasifier: the effect of reaction kinetics and char structure," Fuel, Vol. 79, No. 14, 2000, pp. 1767-1779.
[8] Chen, C.X., M. Horio, and T. Kojima, "Numerical simulation of entrained flow coal gasifiers. Part I: modeling of coal gasification in an entrained flow gasifier," Chemical Engineering Science, Vol. 55, No. 18, 2000, pp. 3861-3874.
[9] Fletcher, D.F., et al., "A CFD based combustion model of an entrained flow biomass gasifier," Applied Mathematical Modelling, Vol. 24, No. 3, 2000, pp. 165-182.
[10] Liu, X.J., W.R. Zhang, and T.J. Park, "Modelling coal gasification in an entrained flow gasifier," Combustion Theory and Modelling, Vol. 5, No. 4, 2001, pp. 595-608.
[11] Vicente, W., et al., "An Eulerian model for the simulation of an entrained flow coal gasifier," Applied Thermal Engineering, Vol. 23, No. 15, 2003, pp. 1993-2008.
[12] Wu, Y.X., et al., "Effects of Turbulent Mixing and Controlling Mechanisms in an Entrained Flow Coal Gasifier," Energy & Fuels, Vol. 24, No., 2010, pp. 1170-1175.
[13] M. Frenklach, H. Wang, C.-L. Yu, M. Goldenberg, C.T. Bowman, R.K. Hanson, D.F. Davidson, E.J. Chang, G.P. Smith, D.M. Golden, W.C. Gardiner and V. Lissianski, http://www.me.berkeley.edu/gri_mech/; and Gas Research Institute Topical Report: M. Frenklach, H. Wang, M. Goldenberg, G.P. Smith, D.M. Golden, C.T. Bowman, R.K. Hanson, W.C. Gardiner and V. Lissianski, 'GRI-Mech---An Optimized Detailed Chemical Reaction Mechanism for Methane Combustion,' Report No. GRI-95/0058, November 1, 1995.
[14] D. Vamvuka, "Modelling of an entrained flow coal gasifier, 1. Development of the model and general predictions," Fuel Vol. 74 No. 10, pp. 1452-1460, 1995.
[15] M.A. Field, Combustion and Flame 13 (1969) 237-248.